Langmuir

Article

pubs.acs.org/Langmuir

Spatial Control over Cross-Linking Dictates the pH-Responsive Behavior of Poly(2-(*tert*-butylamino)ethyl methacrylate) Brushes

Abdullah M. Alswieleh,‡ Nan Cheng,‡ Graham J. Leggett,* and Steven P. Armes*

Department of Chemistry, University of Sheffield, Brook Hill, Sheffield S3 7HF, United Kingdom

Supporting Information

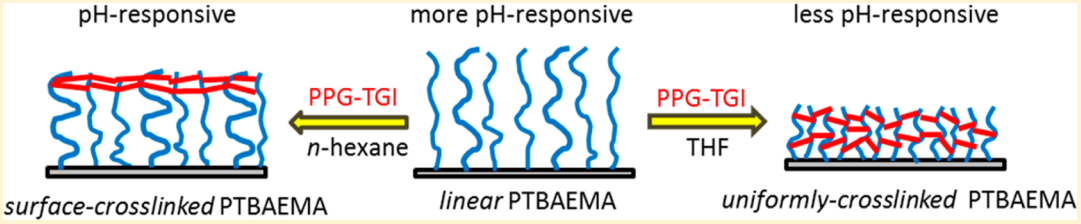

ABSTRACT: Surface-initiated atom transfer radical polymerization (ATRP) of 2-(*tert*-butylamino)ethyl methacrylate (TBAEMA) produced pH-responsive secondary amine-functionalized polymer brushes with dry thicknesses ranging from 4 to 28 nm, as determined by ellipsometry. At low pH, linear PTBAEMA brushes became protonated and highly swollen; brush collapse occurred when the solution pH was increased to ca. 7.7 due to deprotonation. PTBAEMA brushes were subsequently cross-linked using tolylene-2,4-diisocyanate-terminated poly(propylene glycol) (PPG-TGI) in either THF (a good solvent for PTBAEMA) or *n*-hexane (a poor solvent). The intensity of the C−C−O component (286.5 eV) in the C1s X-ray photoelectron spectrum increased after reaction with PPG-TDI, suggesting that cross-linking was successful in both solvents. Ellipsometry studies indicated that the pH-responsive behavior of these cross-linked brushes is dictated by the spatial location of the PPG-TDI cross-linker. Thus, uniformly cross-linked brushes prepared in THF became appreciably less swollen at a given (low) pH than surface-cross-linked brushes prepared in *n*-hexane. Micro- and nanopatterned PTBAEMA brushes were prepared via UV irradiation and interference lithography, respectively, and characterized by atomic force microscopy. The change in brush height was determined as a function of pH, and these AFM observations correlated closely with the ellipsometric studies.

INTRODUCTION

Stimulus-responsive surfaces continue to attract considerable interest since they enable a range of properties such as wettability, stiffness, biocompatibility, frictional coefficients, or specific binding to be regulated and controlled.[1−5] In principle, such "smart" surfaces have diverse potential applications, such as drug delivery,[6−8] aqueous lubrication,[9−11] coatings for biomedical devices,[3,12] and nanoparticle transport.[13−15] In particular, the combination of the so-called "grafting from" process with living radical polymerization techniques such as atom transfer radical polymerization (ATRP)[16,17] has enabled well-defined polymer brushes to be prepared with thicknesses of up to several hundred nanometers from either planar or colloidal substrates.[17−20]

Depending on the chemical composition of such polymer brushes, their conformation can be manipulated using external stimuli[2,5,21,22] such as pH,[23−28] temperature,[27,29−31] solvent,[32] and light[33] or an electrical stimulus.[15,34−36] For example, Okano and co-workers reported that planar substrates coated with thermo-responsive poly(*N*-isopropylacrylamide) brushes enable cell adhesion on the collapsed hydrophobic brush layer at 37 °C with subsequent facile cell detachment on cooling below 32 °C, since the brush becomes highly hydrophilic under these conditions.[37]

One of the most studied classes of stimulus-responsive surfaces is pH-responsive polymer brushes. Ionization (or protonation) of functional groups in the brush structure causes chain extension or collapse, depending on the solution pH in which the brush layer is immersed. For example, both polyacids, such as poly(acrylic acid)[28,38] or poly(methacrylic acid),[39,40] and polybases, such as poly(2-(dimethylamino)ethyl methacrylate),[25,41,42] poly(2-(diethylamino)ethyl methacrylate),[43−45] or poly(2-(diisopropylamino)ethyl methacrylate),[43] have been widely studied by various research groups.

At low pH, weak polybase brushes swell when the counterion contribution to the osmotic pressure exceeds the combinatorial excluded volume contribution.[46,47] Moglianetti et al. reported that PDMAEMA brushes became more swollen below pH 3 as a result of a greater osmotic driving force, causing the brush chains to stretch away from the interface.[46] The fraction of protonated monomer repeat units varied through the brush layer, with lower degrees of protonation within the brush interior.[48] Jia et al. reported that the degree of swelling of PDMAEMA brushes depended on their grafting density, with lower grafting densities displaying higher degrees of swelling.[47]

Received: September 30, 2013
Revised: January 13, 2014
Published: January 13, 2014

   dx.doi.org/10.1021/la403666y | *Langmuir* 2014, 30, 1391−1400

Scheme 1. Schematic Representation of the Nature of the Cross-Linking Produced within a PTBAEMA Brush Layer When Using a PPG-TDI Cross-Linker in Conjunction with a Good Solvent (THF) or a Poor Solvent (*n*-hexane)[a]

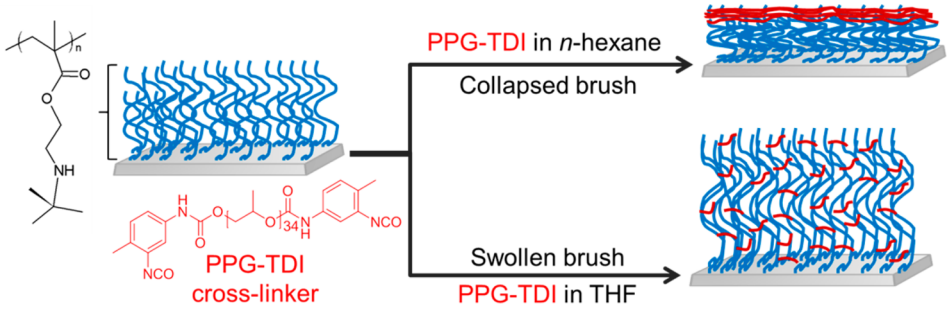

[a]The former solvent results in a uniformly cross-linked brush, whereas the latter results in a surface-cross-linked brush.

There has been very little work focused on secondary amine-functionalized brushes.[49] One commercially available secondary amine-based vinyl monomer is 2-(*tert*-butylamino)ethyl methacrylate (TBAEMA). Well-defined PTBAEMA-based block copolymers have been prepared using living anionic polymerization via sequential monomer addition.[49,50] Morse and co-workers recently prepared well-defined lightly cross-linked PTBAEMA latex particles using aqueous emulsion polymerization.[51] These pH-responsive latexes proved to be effective Pickering emulsifiers for a range of oils when emulsified at pH 10, with demulsification occurring on addition of acid since this caused a latex-to-microgel transition.[51] Jerome and co-workers prepared PTBAEMA-functionalized polyolefin fibers via two protocols.[49,52] In one case, a polyolefin-PTBAEMA diblock copolymer was synthesized by ATRP and dispersed within low-density polyethylene, which led to bactericidal activity toward *E. coli*. In the second study, primary amine-functionalized PTBAEMA chains were prepared via an azide-functional initiator, which led to chemical grafting of the PTBAEMA to maleic anhydride-grafted polypropylene. Dispersion of this graft copolymer within native polypropylene led to long-lasting antibacterial activity. However, to the best of our knowledge, there is very little work on the synthesis and pH-responsive behavior of well-defined PTBAEMA brushes in the literature.

In the present study, uniform PTBAEMA brushes were grown from planar surfaces using surface ATRP. The pH-responsive behavior of these linear brushes was characterized using ellipsometry and compared to that of cross-linked brushes. For example, if stimulus-responsive polymer brushes can be covalently cross-linked while achieving spatial confinement, this is expected to produce more robust surface layers with minimal detrimental effect on their stimulus-responsive character.[53,54] Cross-linking was achieved using a commercially available polymeric diisocyanate, which reacts with the secondary amine groups in the TBAEMA residues. Spatial control was achieved by selecting the solvent used for the cross-linking reaction. Thus, using a good solvent (e.g., THF) for the PTBAEMA brush allows relatively uniform cross-linking throughout the highly swollen brush layer, whereas using a poor solvent (e.g., *n*-hexane) leads to cross-linking being confined to the upper surface of the collapsed brush (see Scheme 1). In principle, such spatial confinement should significantly affect the pH-responsive behavior of the brush layer: this hypothesis is examined using various surface characterization techniques, including in situ ellipsometry, atomic force microscopy (AFM), and X-ray photoelectron spectroscopy (XPS).

EXPERIMENTAL SECTION

Materials. Silicon wafers ([100] orientation, boron-doped, 0−100 Ω cm) were purchased from Compart Technology (Peterborough, U.K.). Deionized water was obtained using an Elga Pure Nanopore 18.2 MΩ system. 3-Aminopropyltriethoxysilane (APTES) (>98%), 2-bromoisobutyryl bromide (BIBB) (98%), and triethylamine (99%) were purchased from Sigma-Aldrich (Gillingham, U.K.). Hydrogen peroxide (30%), sulfuric acid (95%), ethanol (99.8%, HPLC grade), ammonium hydroxide (Analar), dichloromethane (HPLC grade), tetrahydrofuran (THF) (99.5%, HPLC grade), *n*-hexane (HPLC grade), and basic alumina were obtained from Fisher Scientific (Loughborough, U.K.). THF and *n*-hexane were supplied by the Grubbs dry solvent system. Copper(I) bromide (>98%), copper(II) bromide (>99%), tolylene 2,4-diisocyanate-terminated poly(propylene glycol) (PPG-TDI), tris(2-pyridylmethyl)amine (TPMA, 98%), and 2-(*tert*-butylamino)ethyl methacrylate (TBAEMA, 97%) were obtained from Sigma-Aldrich (Gillingham, U.K.). All chemicals were analytical reagent grade and used as received. Copper(I) bromide was stored under vacuum prior to use. TBAEMA was treated with basic alumina to remove inhibitor and stored at 4 °C before use.

Preparation of ATRP Initiator on Silicon Wafers. All glassware and substrates were immersed in "piranha" solution for 2 h. (Caution: *Piranha solution comprises three parts hydrogen peroxide to seven parts concentrated sulfuric acid; it is an extremely strong oxidizing agent that has been known to detonate spontaneously upon contact with organic material*). The treated glassware and substrates were rinsed copiously with deionized water and then sonicated for 10 min, followed by oven drying at 120 °C for 1 h. These clean silicon wafers were then immersed in a 1:1:5 solution of ammonium hydroxide, 30% hydrogen peroxide, and deionized water. This reaction solution was heated to 85 °C for 30 min before being allowed to cool to 20 °C. The treated wafers were rinsed with deionized water, sonicated, and then oven-dried before use.[55,56] A 2.0% v/v ethanolic solution of 3-aminopropyltriethoxysilane (APTES) was aged for 5 min at 20 °C. Silicon wafers were immersed in this APTES solution for 30 min, rinsed with ethanol, dried using a nitrogen gas stream, and annealed for 30 min at 120 °C.[55−57] The resulting amine-functionalized wafers were then immersed in a solution of 2-bromoisobutyryl bromide (BIBB) (0.37 mL, 3 mmol) and triethylamine (0.41 mL, 3 mmol) in dichloromethane (DCM; 60 mL) for 30 min at 20 °C. Subsequently, the initiator-functionalized wafers were rinsed with ethanol and DCM and dried using a nitrogen gas stream prior to use.

Photopatterning of ATRP Initiator-Functionalized Surfaces. A Coherent Innova 300C FreD frequency-doubled argon ion laser (Coherent UK, Ely, U.K.) was used to irradiate samples at a UV wavelength of 244 nm. The laser power was adjusted to be between 1 and 100 mW. The area exposed to the laser beam was 0.06 cm^2. Micropatterns were obtained by irradiation of the 3-(2-bromoisobutyramido)propyl triethoxysilane (BIBAPTES) monolayer on the silicon wafer using an electron microscope copper grid (Agar, Cambridge, U.K.) as a convenient mask.[55,57] Interferometric lithography (IL) was conducted using a two-beam interference system

dx.doi.org/10.1021/la403666y | *Langmuir* 2014, 30, 1391−1400

Scheme 2. (A) Schematic Representation of the Formation of an Amide-Based ATRP Initiator Layer. (B) Synthesis of a Linear PTBAEMA Brush from an Initiator-Functionalized Planar Surface via ATRP in Isopropyl Alcohol at 20 °C

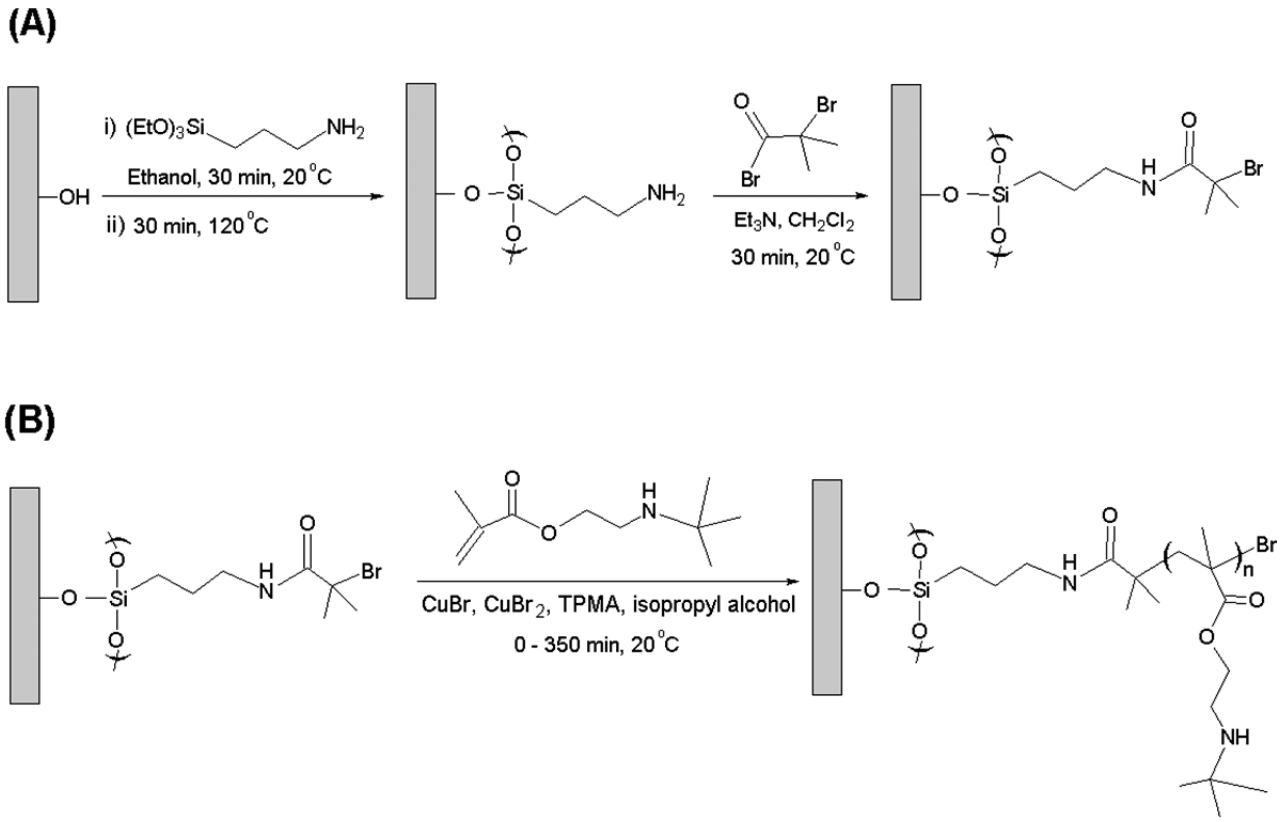

(Lloyd's mirror), as reported elsewhere.[55] Micropatterning was achieved by exposing BIBBAPTES-functionalized silicon wafers to 2.2 J cm^{-2} laser radiation at 244 nm using a 2000 mesh electron microscope grid as a mask. This protocol ensures complete removal of Br atoms.[55] Friction force microscopy (FFM) was used to image the resulting surface patterns. Nanoscale patterning was carried out using IL to achieve photolytic patterning of the BIBBAPTES surface layer on the silicon wafer. A Lloyd's Mirror dual-beam interferometer was utilized whereby a coherent UV laser beam was directed toward a mirror and the sample was placed at an angular separation of 2θ. One-half of the laser beam is incident on the mirror, from where it is reflected onto the sample to interfere with the other half of the beam, forming a sinusoidal intensity pattern with a period of $\lambda/(2 \sin \theta)$, where λ is the laser wavelength of 244 nm. In this experiment, the BIBBAPTES layer was exposed to 0.7 J cm^{-2} at 20 °C. FFM was used to image the BIBBAPTES film .

ATRP Synthesis of PTBAEMA Brushes. TBAEMA (5.0 g, 27 mmol) was dissolved in isopropanol (IPA; 5.0 mL) at 20 °C, deoxygenated for 30 min, and stored under N_2 prior to use. TPMA (58.8 mg, 0.203 mmol) and Cu(II)Br_2 (15.0 mg, 0.068 mmol) were added to the solution and deoxygenated for 20 min, after which Cu(I)Br (19.0 mg, 0.135 mmol) was added and the monomer/catalyst mixture was deoxygenated for a further 10 min. Initiator-coated wafers were sealed in Schlenk tubes and deoxygenated via three vacuum/nitrogen cycles. The monomer/catalyst solution (5 mL) was syringed into each tube under a nitrogen atmosphere, and surface polymerization of TBAEMA was allowed to proceed at 20 °C for a given reaction time. Each polymerization was quenched after the desired reaction time by removing the wafer from its Schlenk tube, followed by washing with IPA and ethanol several times. The same protocol was used for synthesis of patterned PTBAEMA brushes.

Preparation of Cross-Linked PTBAEMA Brushes. Uniformly cross-linked PTBAEMA brushes (with dry brush thicknesses ranging from 4 to 28 nm, as judged by ellipsometry) were prepared by immersing the linear PTBAEMA brush-coated wafers prepared as described: 1 mL of a 1 mg/L stock solution of 2,4-diisocyanate-terminated poly(propylene glycol) (PPG-TDI) in dry THF at 20 °C.

The grafting density (σ) of the PTBAEMA brushes was calculated from the dry brush thickness (h) using $\sigma = \rho h N_A/M_n$, where ρ is the density of PTBAEMA (~1.1 g cm^{-3}),[51] N_A is Avogadro's number, and M_n is the number-average molecular weight. While the thickness h is readily determined by ellipsometry, M_n values are not available. However, following established literature protocols,[27] we also synthesized soluble (nongrafted) PTBAEMA chains in the bulk solution using a soluble initiator while simultaneously growing brushes from an initiator-modified planar silicon wafer. If we assume that the rate of polymerization in solution is the same as that on the planar surface,[58,59] this allows the relationship between the M_n of the soluble PTBAEMA chains (determined by GPC) and the ellipsometric brush thickness (h) for the PTBAEMA brush to be established. This approximate method has been used by other groups,[60,61] even though it is known that the M_n of solution-grown polymers is not precisely the same as that of polymer brushes grown from planar surface.[62] GPC analysis of free PTBAEMA chains grown in solution indicates an M_n of 12 700 g mol^{-1} (vs poly(methyl methacrylate) standards). A PTBAEMA brush of 10 nm dry thickness grown in the same reaction solution is assumed to have the above M_n value (hence, the likely systematic error incurred by using inappropriate GPC standards is ignored in this analysis). On this basis, the brush grafting density was calculated to be 0.55 chains nm^{-2}. For this 10 nm PTBAEMA brush grown from a 1 cm^2 area of silicon wafer (9.7×10^{-9} mol) we used 1.0 mL of a 1.0 mg dm^{-3} stock solution of 2,4-diisocyanate-terminated poly(propylene glycol) (PPG-TDI) (4.34×10^{-10} mol) for the cross-linking reaction; thus, we calculate that there are approximately 22 secondary amine groups per isocyanate. Given that some fraction of the isocyanate groups is likely to be wasted via intramolecular reaction with secondary amine groups on the same brush chain (as opposed to the desired intermolecular cross-linking reaction), this is considered to be an upper limit value.

dx.doi.org/10.1021/la403666y | Langmuir 2014, 30, 1391−1400

This protocol ensures that the brush layer is not overcross-linked, so that it retains some degree of stimulus-responsive behavior. After 10 min, the wafer was rinsed copiously with THF to remove any unreacted PPG-TDI cross-linker and dried under a stream of nitrogen gas. The same protocol was utilized to prepare surface-cross-linked PTBAEMA brushes, except that dry *n*-hexane was used instead of THF.

Surface Characterization. Ellipsometric studies were conducted using a Alph-SE ellipsometer (J. A. Woollam Co., Lincoln, NE) equipped with a He−Ne laser (λ = 633 nm) at an incident angle (Φ) of 70° from the normal. Ellipsometric thicknesses were calculated from silicon substrate models. Measurements were conducted from 300 to 700 nm, and modeling was performed using WVASE software (J. A. Woollam Co., USA). Fit quality was assessed using the root-mean-square error (RMSE) between the measured and the modeled ellipsometric constants Δ and Ψ over all measured wavelengths. The dry films were modeled as a single layer of variable thickness with refractive index given by the Cauchy parameters of A_n = 1.5 μm^2 and B_n = 0.005 μm^2 (found by fitting these values for a thick PTBAEMA film). The ellipsometric brush thickness for each sample was determined in at least three different places on the wafer and reported as the mean ± standard error.[63] In situ measurements of brush thickness in aqueous solution were conducted using a homemade liquid cell. The sample cell was rinsed several times with deionized water between each measurement. Ellipsometric data were fitted using a single-slab model with a refractive index given by a linear effective medium approximation (EMA) between the PTBAEMA brush and water.[43,64] Again, three measurements were recorded for each brush sample and reported as the mean ± standard error.

AFM measurements were conducted using a Digital Instruments Nanoscope IV Multimode Atomic Force Microscope (Veeco, Santa Barbara, CA) with a 'J' scanner (0−125 μm). Silicon nitride nanoprobes (Digital Instruments, Cambridge, U.K.) with nominal spring constants of either 0.06 or 0.12 N m^{-1} and tip radii of 20−60 nm were used for contact mode imaging. Silicon probes with nominal spring constants ranging from 20 to 80 N m^{-1} were used for tapping mode imaging. All samples were allowed to stand in the liquid cell for at least 5 min prior to any measurements in order to attain equilibrium. Mean heights were determined for both dry micro- and nanopatterned brushes in air and also for swollen brushes immersed in pH buffer solutions ranging from pH 2 to 12.

X-ray photoelectron spectroscopy was carried out using a Kratos Axis Ultra spectrometer (Kratos Analytical, Manchester, U.K.) with a monochromatic Al Kα X-ray source operating at a power of 150 W with an emission current of 8 mA. The base pressure in the spectrometer was typically 10^{-8}−10^{-10} mbar. Electron energy analyzer pass energies of 20 and 160 eV were used to acquire core-line spectra and survey scans, respectively. The energy resolution for the wide scans was 1.0 eV. This was reduced to 0.1 eV for high-resolution scans. Core-line spectra were peak-fitted using Casa XPS software, and all binding energies were referenced relative to the main hydrocarbon C1s signal calibrated at 285 eV.

A Malvern Zetasizer NanoZS model ZEN 3600 instrument equipped with a Malvern streaming potential cell attachment was used to measure the surface zeta potential of these polymer brushes. Surface zeta potentials were measured at 25 °C in the presence of 1 mM KCl using a sterically stabilized polystyrene latex as non-interacting tracer particles. The steric stabilizer was selected to be a highly hydrophilic zwitterionic polymer, namely, poly(2-(methacryloyloxy)ethyl phosphorylcholine) (PMPC). A PMPC-stabilized polystyrene latex was synthesized as reported previously by Armes and co-workers.[65]

RESULTS AND DISCUSSION

Brush Formation and Cross-Linking. The first stage in brush synthesis was functionalization of a silica surface with 3-aminopropyltriethoxysilane (see Scheme 2A). The surface amine groups were subsequently converted into 2-bromoisobutyryl amide initiator sites by reaction with excess 2-bromoisobutyryl bromide. The resulting films were characterized by XPS (see Figures S1A and S1B, Supporting Information). Their C1s spectra exhibited the expected features.[55] PTBAEMA brushes were prepared by surface ATRP (Scheme 2B). This living radical polymerization technique has been widely used to grow polymer brushes.[16,17,66] In particular, Ding et al. reported[67] the rather slow growth of PTBAEMA brushes from a planar silicon substrate via living radical polymerization. An ATRP formulation involved using a CuCl/$CuCl_2$/HMTETA catalyst at 90 °C in the bulk, whereas a single electron transfer living radical polymerization (SET-LRP) formulation employed Cu(0) in DMSO at 75 °C.[67] The former protocol produced a relatively well-defined brush of around 20 nm dry thickness after 72 h, while the latter gave a less uniform brush of approximately 17 nm after 96 h. However, no detailed information regarding the kinetics of PTBAEMA brush growth was reported for either formulation, and perhaps surprisingly, the pH-responsive behavior of such brushes was not investigated.

Various formulations were examined in the present work, including different combinations of ligand, catalyst, solvent, and temperature. The objective was to identify a suitable formulation that would allow well-controlled PTBAEMA brush growth to be achieved within a few hours at 20 °C. Empirically, it was found that a suitable ATRP formulation comprised Cu(I)Br, Cu(II)Br_2, and TPMA ligand in IPA, with a [TBAEMA]:[CuBr]:[$CuBr_2$]:[TPMA] relative molar ratio of 200:1:0.5:1.5. Figure 1 shows the PTBAEMA brush dry thickness as a function of polymerization time using this optimized protocol. A linear growth regime was observed from 15 to 125 min, with departure from linearity between ~150 and 350 min as the rate of surface polymerization becomes retarded. The latter regime is most likely indicative of premature chain termination.

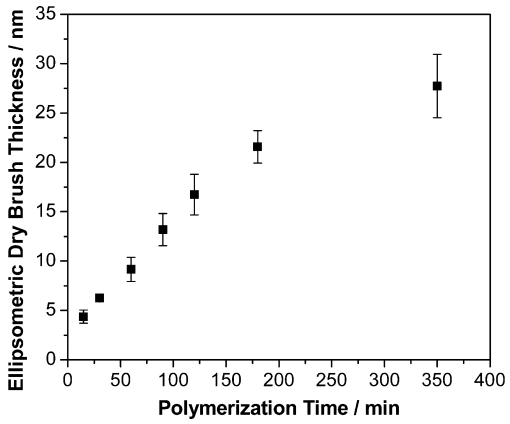

Figure 1. Evolution of ellipsometric dry brush thickness versus polymerization time for growth of linear PTBAEMA brushes prepared via surface ATRP in isopropyl alcohol at 20 °C. Conditions: [TBAEMA]:[CuBr]:[$CuBr_2$]:[TPMA] molar ratio = 200:1.0:0.5:1.5.

Brushes were cross-linked using tolylene 2,4-diisocyanate-terminated poly(propylene glycol) (PPG-TDI) dissolved in either THF or *n*-hexane. The molar ratio of secondary amine (from PTBAEMA brushes) to isocyanate end-groups (from PPG-TDI) was approximately 22. This ensures that the brush layer is not over-cross-linked, so that it retains its stimulus-responsive behavior after cross-linking.

XPS is a surface-specific analysis technique with a sampling depth of around 10 nm. The elemental compositions of the linear, uniformly cross-linked, and surface-cross-linked PTBAEMA brushes are presented in Table 1. The dry brush thickness was 18 nm in each case. For linear PTBAEMA brushes, the elemental compositions (C, N, O) were similar to the calculated values (C = 77.0%, N = 7.6%, and O = 15.3%). After cross-linking, the O/N atomic ratio increased because of the introduction of O atoms in the PPG-TDI cross-linker. The O/N atomic ratio increased for the surface-cross-linked PTBAEMA brushes, suggesting that there is a higher degree of cross-linking at the brush surface. These observations are consistent with the hypothesis that PPG-TDI cross-linking conducted using a poor solvent (*n*-hexane) yields cross-linking that is predominantly confined to the upper surface of the brush layer. There is a higher O/N atomic ratio for the uniformly cross-linked brushes prepared in THF compared to the linear brush.

Table 1. XPS Data Summarizing the Elemental Compositions of the Linear PTBAEMA Brush, Uniformly Cross-Linked PTBAEMA Brush, and Surface-Cross-Linked PTBAEMA Brush

sample description	% C	% N	% O
linear PTBAEMA brush	79.52	6.99	13.49
PTBAEMA brush surface-cross-linked in *n*-hexane	76.49	3.94	19.57
PTBAEMA brush uniformly cross-linked in THF	78.63	6.12	15.24

The C1s spectrum of an as-prepared PTBAEMA brush is shown in Figure 2A. The peaks corresponding to hydrocarbon carbon atoms at 285.0 eV (−C−C−C−) and to the carbon atoms adjacent to nitrogen at 285.8 eV (−C−C−NH−) were separated by an energy difference close to that of the resolution of the spectrometer; hence they were fitted using a single component. Separate components were included to account for the −C−C−O− signal at 286.4 eV and the ester carbonyl component at 288.9 eV. The respective relative peak areas after fitting were 5.7:2.41:1, which are in reasonable agreement with the calculated theoretical ratio of 6:3:1.

The C1s spectrum of a PTBAEMA brush after surface cross-linking in *n*-hexane is presented in Figure 2B. A substantial increase in intensity is observed for the C−C−O component at 286.4 eV. This is attributed to the presence of additional C−O bonds contributed by the PPG-TDI cross-linker (which confers 34 polymerized propylene glycol units per cross-link). The actual degree of cross-linking cannot be determined easily, since some unknown fraction of the PPG-TDI reagent is likely to also react with two N−H bonds on the same PTBAEMA chain to form an intramolecular cycle, rather than forming an intermolecular cross-link.

Cross-linking the PTBAEMA brush in THF (Figure 2C) also led to an increase in the contribution from the C−C−O component. However, this change was smaller than that observed after cross-linking in *n*-hexane. Given that the XPS sampling depth is ca. 10 nm, these data are consistent with the hypothesis that using PPG-TDI in combination with a good solvent (THF) yields more extensive uniform cross-linking within the brush layer (and hence a somewhat lower extent of surface cross-linking). Thus the cross-links are concentrated within the XPS sampling depth for collapsed brushes cross-linked in *n*-hexane, but are distributed more uniformly throughout the brush layer when cross-linking is conducted in THF; hence, only some fraction of the cross-links are located within the XPS sampling depth in the latter case.

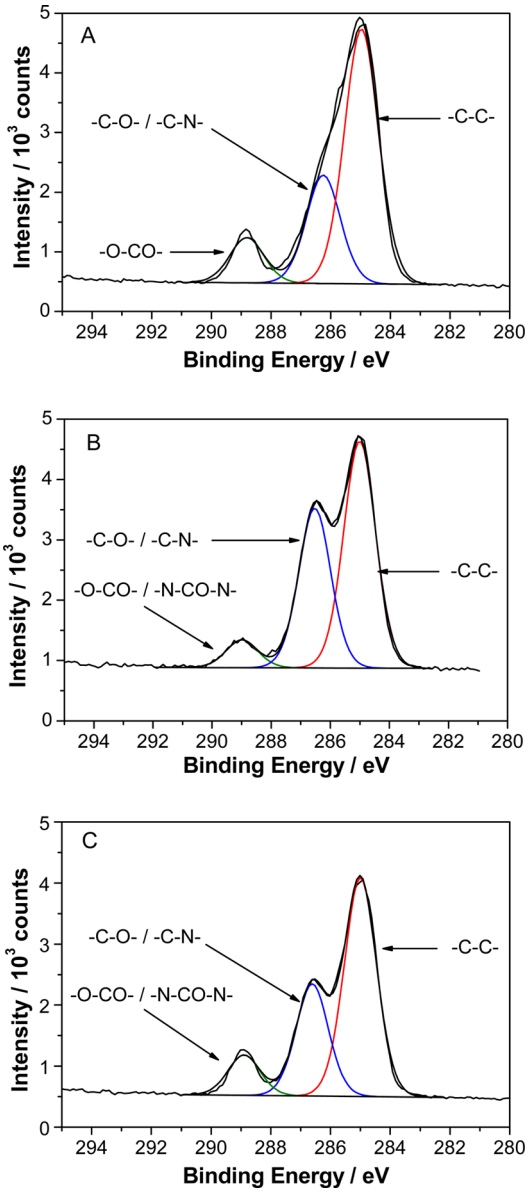

Figure 2. X-ray photoelectron core-line spectra recorded for a series of PTBAEMA brushes (each of 18 nm dry thickness). (A) C1s spectrum obtained for a linear PTBAEMA brush. (B) C1s spectrum obtained for the same surface-cross-linked PTBAEMA brush prepared using PPG-TDI in *n*-hexane. (C) C1s spectrum obtained for the same uniformly cross-linked PTBAEMA brush prepared using PPG-TDI in THF.

Sample Topography. Tapping-mode AFM height images of linear and cross-linked PTBAEMA brushes grown from planar silicon wafers (~15 nm dry brush thickness) were acquired by AFM (Figure S2, Supporting Information). A modest increase in the root-mean-square roughness was observed after cross-linking, but the extent of this change was not statistically significant.

Patterning. Micropatterned PTBAEMA brushes were prepared by exposure to UV light through a mask. Previous studies have demonstrated that exposure to UV light causes debromination of the initiator, rendering it inactive for subsequent ATRP.[55] In friction images of the patterned initiator (Figure S3A, Supporting Information), high contrast

dx.doi.org/10.1021/la403666y | *Langmuir* 2014, 30, 1391−1400

was observed between the masked regions (dark contrast) and exposed regions (light contrast). The contrast difference arises from the more polar nature of the exposed regions, leading to a stronger adhesive interaction with the AFM probe and hence a greater rate of energy dissipation and a larger friction force. Figure 3 shows a tapping-mode AFM height image recorded for

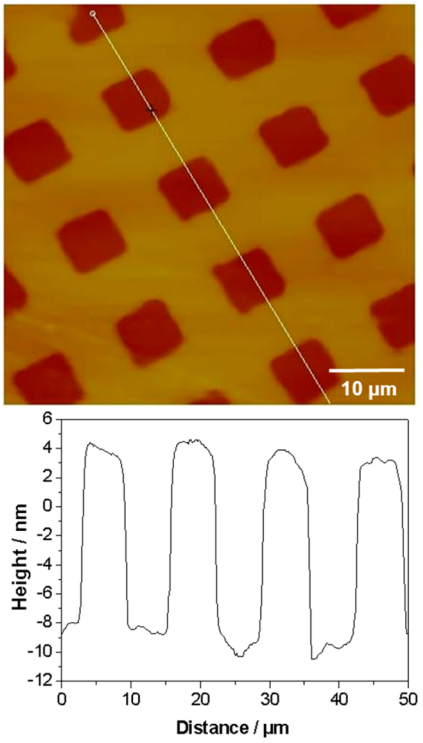

Figure 3. Tapping-mode AFM studies of the periodic brush height recorded for a micropatterned linear PTBAEMA brush: topographical image (left), cross-section analysis (right). Image size: 50 × 50 μm.

a PTBAEMA brush film grown from a micropatterned substrate prepared as described above. Brighter regions correspond to the brush layer, whereas darker regions correspond to the exposed regions where no brush growth occurs because of photolysis of the C−Br bond in the surface-bound initiator sites. The mean brush thickness can be determined by measuring the height difference between the masked and the exposed regions in the image.

PTBAEMA brushes were also obtained by growing brushes from nanopatterned ATRP initiators fabricated by exposure to UV light in an interferometer. A typical friction force microscopy (FFM) image is presented in Figure S3B (see Supporting Information). The bright bands of 160 ± 7 nm full width at half-maximum (fwhm) correspond to areas of extensive surface modification, resulting from exposure to maxima in the interferogram, whereas the dark bands of 140 ± 6 nm (fwhm) correspond to regions of little or no surface modification that were exposed to minima in the interferogram. The tapping-mode AFM topographical image confirmed that there was no height contrast, indicating that no removal of material had occurred (Figure 4). It was observed that brushes grown from such nanopatterns were significantly thinner than brushes grown from micropatterns under the same conditions. For example, the tapping-mode AFM topographical image of nanopatterned PTBAEMA brushes indicated a mean brush height of 4.5 ± 0.5 nm, whereas for micropatterned PTBAEMA

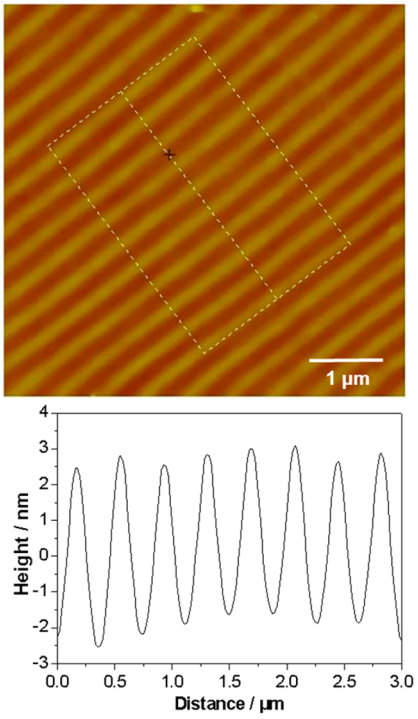

Figure 4. Tapping-mode AFM studies of the periodic brush height recorded for a nanopatterned linear PTBAEMA brush: topographical image (left), cross-section analysis (right). Image size: 5 × 5 μm^2.

brushes grown under identical conditions the average brush height was about 14 ± 3 nm. Kaholek et al. also reported a reduction in brush height on reducing the feature size of the pattern.[55,68] These workers hypothesized that "at constant grafting density a polymer brush in good solvent adopts a vertically less ordered and laterally more extended conformation, induced by the lack of lateral restraint the brush experiences at its boundaries, leading to less chain crowding and thus less chain stretching." Polymer structures grown from finer patterns are also likely to be more relaxed (less brush-like) near the edges of the pattern, resulting in thinner polymer brushes even in the dry state.

pH-Responsive Behavior. The secondary amine groups presented in the weakly basic PTBAEMA brushes are readily protonated when immersed in acidic solution.[51] The resulting cationic brushes become highly swollen and stretch away from the surface because of the strong lateral electrostatic repulsive forces between adjacent chains. According to the literature,[61] swelling of polymer brushes may be attributed to two factors: a combinatorial excluded volume effect and a counterion-induced osmotic pressure. The former term is significantly reduced via chemical or physical cross-linking,[53,54,69] but the latter term remains relatively unaffected. For example, Moglianetti et al. studied[61,69] the interaction between PDMAEMA brushes and sodium dodecyl sulfate (SDS) in both acidic and alkaline media. A reduction in PDMAEMA brush swelling after physical cross-linking using SDS surfactant was attributed to annealing of the excluded volume.[69] The pH-responsive behavior of PTBAEMA brushes grown from silicon wafers was investigated by immersion in aqueous buffers ranging from pH 2 to 12. In acidic aqueous solution, the brushes become fully protonated and attain their maximum swollen thickness. In alkaline media, PTBAEMA brushes gradually become deprotonated and hence adopt their collapsed conformation. This pH-modulated brush

dx.doi.org/10.1021/la403666y | Langmuir 2014, 30, 1391−1400

thickness for chemically cross-linked and non-cross-linked (linear) PTBAEMA brushes was studied using both ellipsometry (see Figure 5) and AFM (see Figure 6).

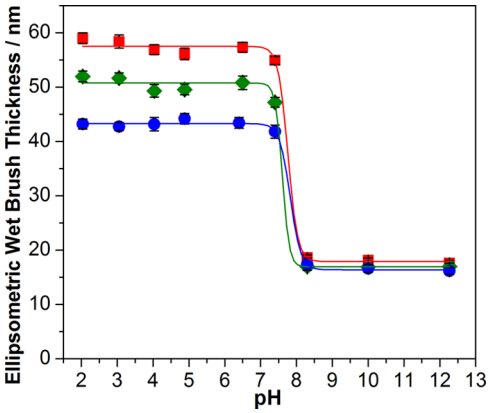

Figure 5. In situ ellipsometric thickness of PTBAEMA brushes immersed in aqueous solution as a function of solution pH. (■) Linear PTBAEMA brush (original dry thickness = 16 nm). (●) Same PTBAEMA brush uniformly cross-linked in THF using PPG-TDI at 20 °C. (♦) Same PTBAEMA brush surface cross-linked in *n*-hexane using PPG-TDI at 20 °C.

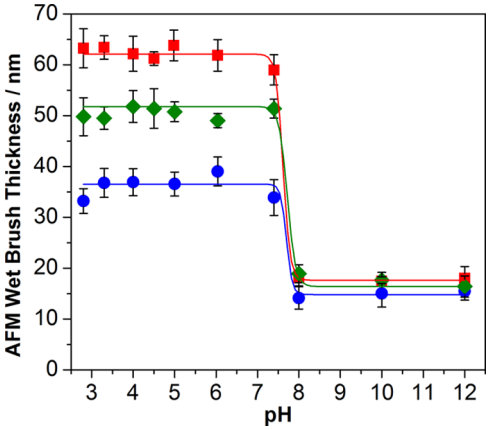

Figure 6. In situ brush height determined by tapping-mode AFM as a function of solution pH for micropatterned PTBAEMA brushes: (■) linear PTBAEMA brush (original dry brush thickness = 15 nm); (●) uniformly cross-linked PTBAEMA brush prepared using PPG-TDI in THF; (♦) surface-cross-linked PTBAEMA brush prepared using PPG-TDI in *n*-hexane.

All brushes exhibited similar thicknesses when collapsed in the dry state and in alkaline media. However, under acidic conditions, the degree of swelling varied with the nature of the normal distribution of the covalent cross-links between chains. Figure 5 shows that the mean thickness of a linear PTBAEMA brush increased from ca. 16 (in the dry state) to 58 nm below pH 8. Above pH 8, the PTBAEMA chains became deprotonated and collapsed to give a brush layer of ca. 18 nm thickness, which is close to the dimensions of the dry brush. Thus the linear swelling factor (the ratio of the thickness of the swollen brush to that of the collapsed brush) is ca. 3.3. The mean thickness of a uniformly cross-linked PTBAEMA brush (prepared using PPG-TDI in THF) increased from 17 nm in alkaline media to 43 nm in acidic solution, corresponding to a linear swelling factor of ca. 2.5. Thus uniform cross-linking throughout the brush layer imposes a significant constraint on its pH-responsive behavior, as expected. This is attributed to the multiple cross-links between the PTBAEMA chains, which restrict the chain mobility. In contrast, for the surface-cross-linked PTBAEMA brush prepared using PPG-TDI in *n*-hexane, the brush thickness increased from 17 nm when immersed in alkaline media to approximately 51 nm in acidic solution, which corresponds to a linear swelling factor of 3.0. Thus the surface-cross-linked PTBAEMA brushes exhibit similar pH-responsive behavior to the linear PTBAEMA brushes. This is because the PPG-TDI cross-linker barely penetrates the collapsed brush layer and hence can only react with the secondary amine groups present in its outer surface. An extensive cross-link network is not created within the brush layer under these conditions; hence this surface-confined cross-linking has rather less effect on the swelling/collapse behavior of the brush compared to uniformly cross-linked brushes.

AFM studies of the micropatterned linear, uniformly cross-linked, and surface-cross-linked PTBAEMA brushes were conducted (see Figure 6 and Figure S4, Supporting Information). As expected, the linear PTBAEMA brushes exhibited the strongest pH-responsive behavior: the mean brush height difference increased from 18 nm for the collapsed state (above pH 8) to 64 nm for the fully stretched brush (below pH 8). This indicates a linear swelling ratio of approximately 3.6. In contrast, the uniformly cross-linked PTBAEMA brushes swelled from 15 (above pH 8) to 36 nm (below pH 7). Again, the surface-cross-linked PTBAEMA brushes exhibited intermediate behavior, with a swollen brush height of 51 nm and a collapsed brush height of 18 nm, indicating a linear swelling ratio of 2.9. These data are in good agreement with the ellipsometric data discussed above, thus confirming that the pH-responsive behavior of PTBAEMA brushes can be modulated by conducting cross-linking in either a good or a bad solvent. The resulting 3D (or 2D) cross-link networks dictate the observed pH-responsive brush behavior, with greater cross-linking restricting the pH response.

The effect of spatially-confined cross-linking was also studied for nanopatterned brushes (Figure S5, Supporting Information). Thus the same AFM experiments were conducted on nanopatterned linear, uniformly cross-linked, and surface-cross-linked PTBAEMA brushes (see Figure 7). Very similar pH-

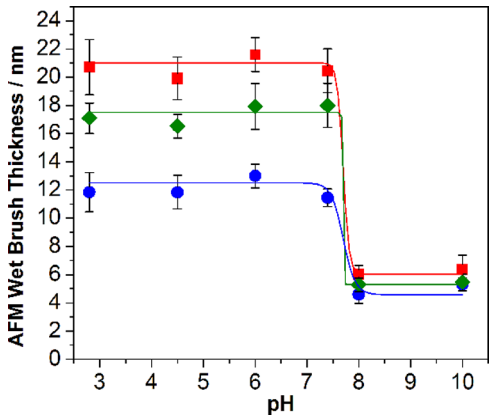

Figure 7. In situ tapping-mode AFM brush height determined as a function of solution pH for nanopatterned PTBAEMA brushes immersed in aqueous solution: (■) linear PTBAEMA brush (original dry brush thickness = 4.5 ± 0.5 nm); (●) uniformly cross-linked PTBAEMA brush prepared using PPG-TDI in THF; (♦) surface-cross-linked PTBAEMA brush prepared using PPG-TDI in *n*-hexane.

dx.doi.org/10.1021/la403666y | *Langmuir* 2014, 30, 1391−1400

reponsive behavior was observed for the three brush types compared to the micropatterned brushes discussed above, except that the pH response was somewhat weaker for the nanopatterned brushes. This is probably because, for such small features, the brush chains are more likely to deform at the periphery of the patterned feature; hence brush-like chain stretching normal to the surface is likely to be attenuated. It is perhaps worth emphasizing that the critical pH for the brush collapse/swelling transition is always observed at around pH 7−8. Further systematic studies within a relatively narrow pH window (see Figure 7) suggest that the brush swelling transition actually occurs between pH 7.6 and 7.8, which is a little lower than the pK_a of approximately 8.0 recently reported for linear PTBAEMA homopolymer in dilute aqueous solution by Morse and co-workers.[51] Covalent cross-linking of the brush chains using PPG-TDI appears to have rather little effect on the effective pK_a of the PTBAEMA brushes described in this study (see Figure 8). Similar observations have been reported by other workers for PDMAEMA brushes.[46,70]

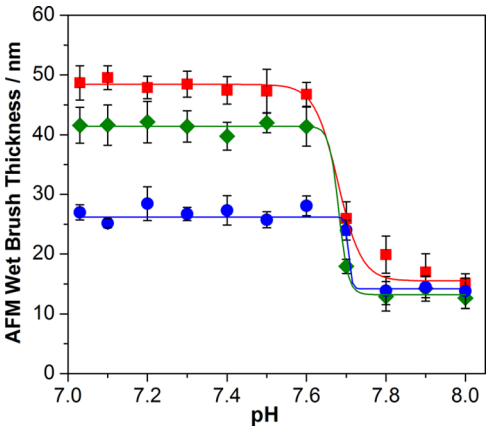

Figure 8. In situ tapping-mode AFM brush height determined over a relatively narrow pH window for micropatterned PTBAEMA brushes immersed in aqueous solution: (■) linear PTBAEMA brush (original dry brush thickness = 13 nm); (●) uniformly cross-linked PTBAEMA brush prepared using PPG-TDI in THF; (♦) surface-cross-linked PTBAEMA brush prepared using PPG-TDI in *n*-hexane.

The surface zeta potentials of linear and cross-linked PTBAEMA brushes were determined from pH 3 to 10 (see Figure S6, Supporting Information). As expected, surface zeta potentials for linear PTBAEMA brushes were +45 ± 5 mV at pH ≤ 7, with a gradual reduction in zeta potential being observed at higher pH as the secondary amine groups become progressively more deprotonated. As expected, the surface zeta potential is reduced after cross-linking because of the reduction in the number of secondary amine groups in the brush layer. Moreover, the surface zeta potential of the surface-cross-linked PTBAEMA brush is somewhat less cationic than that of the uniformly cross-linked PTBAEMA brush.

CONCLUSIONS

Linear PTBAEMA brushes of up to 28 nm dry thickness have been prepared via surface ATRP at 20 °C. Ellipsometric studies confirm that such brushes exhibit pH-responsive behavior, as expected. Highly swollen cationic protonated brushes are produced at low pH, with collapsed neutral deprotonated brushes being obtained above a critical pH of approximately pH 7.7. PTBAEMA brushes can be readily cross-linked via their secondary amine groups using a commercially available polymeric diisocyanate (PPG-TDI) to produce robust urea bonds. XPS studies confirmed the presence of the reacted PPG-TDI cross-linker within the PTBAEMA brush layers. Moreover, the choice of solvent determines the spatial location of this cross-linking reaction. Using THF, which is a good solvent for PTBAEMA, leads to relatively uniform cross-linking throughout the swollen brush layer. On the other hand, conducting the same cross-linking reaction in *n*-hexane, which is a poor solvent for PTBAEMA, leads to surface cross-linking of the collapsed brush layer. This spatial confinement profoundly affects the subsequent pH-responsive behavior of the latter brush layer, which becomes significantly more swollen when immersed in acidic solution than the former uniformly cross-linked brush layer, as judged by ellipsometry studies. However, brush swelling occurs at approximately pH 7.7 regardless of the spatial location of the cross-linking reaction, which is essentially the same critical pH as that found for the linear brush. However, this critical pH is slightly lower than the pK_a of around 8.0 reported for linear PTBAEMA chains.[51] These findings are corroborated by brush heights determined by AFM measurements on either micro- or nanopatterned PTBAEMA brushes prepared via UV laser irradiation or interferometric lithography. In summary, this study provides some interesting new perspectives for the design of pH-responsive polymer brushes.

ASSOCIATED CONTENT

Supporting Information

Synthesis details for soluble PTBAEMA via ATRP, XPS data and friction force images for the BIBAPTES initiator-functionalized silicon wafers, AFM characterization of brush layers before and after cross-linking, AFM height images of micro- and nanopatterned PTBAEMA brushes immersed in aqueous solution at various pH values, surface zeta potential vs pH curves for the linear, uniformly cross-linked, and surface-cross-linked brushes. This material is available free of charge via the Internet at http://pubs.acs.org.

AUTHOR INFORMATION

Corresponding Authors

*E-mail: graham.leggett@shef.ac.uk.
*E-mail: s.p.armes@shef.ac.uk.

Author Contributions

‡These authors contributed equally.

Notes

The authors declare no competing financial interest.

ACKNOWLEDGMENTS

The Saudi Arabian government is thanked for funding a Ph.D. studentship for A.A. G.J.L. thanks EPSRC for a Programme Grant (EP/I012060/1). S.P.A. acknowledges the ERC for an Advanced Investigator Grant (PISA 320372).

REFERENCES

(1) Barbey, R.; Lavanant, L.; Paripovic, D.; Schuwer, N.; Sugnaux, C.; Tugulu, S.; Klok, H. A. Polymer Brushes via Surface-Initiated Controlled Radical Polymerization: Synthesis, Characterization, Properties, and Applications. *Chem. Rev.* **2009**, *109*, 5437−5527.

(2) Stuart, M. A. C.; Huck, W. T. S.; Genzer, J.; Mueller, M.; Ober, C.; Stamm, M.; Sukhorukov, G. B.; Szleifer, I.; Tsukruk, V. V.; Urban, M.; Winnik, F.; Zauscher, S.; Luzinov, I.; Minko, S. Emerging applications of stimuli-responsive polymer materials. *Nat. Mater.* **2010**, *9*, 101−113.

(3) Mendes, P. M. Stimuli-responsive surfaces for bio-applications. *Chem. Soc. Rev.* **2008**, *37*, 2512−2529.
(4) Chen, T.; Ferris, R.; Zhang, J. M.; Ducker, R.; Zauscher, S. Stimulus-responsive polymer brushes on surfaces: Transduction mechanisms and applications. *Prog. Polym. Sci.* **2010**, *35*, 94−112.
(5) Liu, F.; Urban, M. W. Recent advances and challenges in designing stimuli-responsive polymers. *Prog. Polym. Sci.* **2010**, *35*, 3−23.
(6) Liu, H.-B.; Yan, Q.; Wang, C.; Liu, X.; Wang, C.; Zhou, X.-H.; Xiao, S.-J. Saccharide- and temperature-responsive polymer brushes grown on gold nanoshells for controlled release of diols. *Colloids Surf., A* **2011**, *386*, 131−134.
(7) Motornov, M.; Tam, T. K.; Pita, M.; Tokarev, I.; Katz, E.; Minko, S. Switchable selectivity for gating ion transport with mixed polyelectrolyte brushes: approaching 'smart' drug delivery systems. *Nanotechnology* **2009**, *20*.
(8) Bajpai, A. K.; Shukla, S. K.; Bhanu, S.; Kankane, S. Responsive polymers in controlled drug delivery. *Prog. Polym. Sci.* **2008**, *33*, 1088−1118.
(9) Chen, M.; Briscoe, W. H.; Armes, S. P.; Klein, J. Lubrication at Physiological Pressures by Polyzwitterionic Brushes. *Science* **2009**, *323*, 1698−1701.
(10) Raviv, U.; Giasson, S.; Kampf, N.; Gohy, J. F.; Jerome, R.; Klein, J. Lubrication by charged polymers. *Nature* **2003**, *425*, 163−165.
(11) Kobayashi, M.; Terada, M.; Takahara, A. Polyelectrolyte brushes: a novel stable lubrication system in aqueous conditions. *Faraday Discuss.* **2012**, *156*, 403−412.
(12) Alexander, C.; Shakesheff, K. M. Responsive polymers at the biology/materials science interface. *Adv. Mater.* **2006**, *18*, 3321−3328.
(13) Dunderdale, G. J.; Howse, J. R.; Fairclough, J. P. A. Controlling the Motion and Placement of Micrometer-Sized Metal Particles Using Patterned Polymer Brush Surfaces. *Langmuir* **2011**, *27*, 11801−11805.
(14) Dunderdale, G.; Howse, J.; Fairclough, P. pH-Dependent Control of Particle Motion through Surface Interactions with Patterned Polymer Brush Surfaces. *Langmuir* **2012**, *28*, 12955−12961.
(15) Dunderdale, G.; Fairclough, J. P. A. Coupling pH-Responsive Polymer Brushes to Electricity: Switching Thickness and Creating Waves of Swelling or Collapse. *Langmuir* **2013**, *29*, 3628−3635.
(16) Matyjaszewski, K.; Xia, J. Atom transfer radical polymerization. *Chem. Rev* **2001**, *101*, 2921−2990.
(17) Matyjaszewski, K.; Miller, P. J.; Shukla, N.; Immaraporn, B.; Gelman, A.; Luokala, B. B.; Siclovan, T. M.; Kickelbick, G.; Vallant, T.; Hoffmann, H.; Pakula, T. Polymers at Interfaces: Using Atom Transfer Radical Polymerization in the Controlled Growth of Homopolymers and Block Copolymers from Silicon Surfaces in the Absence of Untethered Sacrificial Initiator. *Macromolecules* **1999**, *32*, 8716−8724.
(18) Pyun, J.; Kowalewski, T.; Matyjaszewski, K. Synthesis of polymer brushes using atom transfer radical polymerization. *Macromol. Rapid Commun.* **2003**, *24*, 1043−1059.
(19) Edmondson, S.; Osborne, V. L.; Huck, W. T. S. Polymer brushes via surface-initiated polymerizations. *Chem. Soc. Rev.* **2004**, *33*, 14.
(20) Chen, X. Y.; Armes, S. P. Surface polymerization of hydrophilic methacrylates from ultrafine silica sols in protic media at ambient temperature: A novel approach to surface functionalization using a polyelectrolytic macroinitiator. *Adv. Mater.* **2003**, *15*, 1558−+.
(21) Roy, D.; Cambre, J. N.; Sumerlin, B. S. Future perspectives and recent advances in stimuli-responsive materials. *Prog. Polym. Sci.* **2010**, *35*, 278−301.
(22) Chen, T.; Ferris, R.; Zhang, J.; Ducker, R.; Zauscher, S. Stimulus-responsive polymer brushes on surfaces: Transduction mechanisms and applications. *Prog. Polym. Sci.* **2010**, *35*, 94−112.
(23) Dong, R.; Lindau, M.; Ober, C. K. Dissociation Behavior of Weak Polyelectrolyte Brushes on a Planar Surface. *Langmuir* **2009**, *25*, 4774−4779.
(24) Toomey, R.; Tirrell, M. Functional polymer brushes in aqueous media from self-assembled and surface-initiated polymers. *Annu. Rev. Phys. Chem.* **2008**, *59*, 493−517.
(25) Sanjuan, S.; Perrin, P.; Pantoustier, N.; Tran, Y. Synthesis and swelling behavior of pH-responsive polybase brushes. *Langmuir* **2007**, *23*, 5769−5778.
(26) Zhou, F.; Huck, W. T. S. Three-stage switching of surface wetting using phosphate-bearing polymer brushes. *Chem. Commun.* **2005**, 5999−6001.
(27) Biesalski, M.; Johannsmann, D.; Ruhe, J. Synthesis and swelling behavior of a weak polyacid brush. *J. Chem. Phys.* **2002**, *117*, 4988−4994.
(28) Treat, N. D.; Ayres, N.; Boyes, S. G.; Brittain, W. J. A facile route to poly(acrylic acid) brushes using atom transfer radical polymerization. *Macromolecules* **2006**, *39*, 26−29.
(29) Jonas, A. M.; Glinel, K.; Oren, R.; Nysten, B.; Huck, W. T. S. Thermo-responsive polymer brushes with tunable collapse temperatures in the physiological range. *Macromolecules* **2007**, *40*, 4403−4405.
(30) Azzaroni, O.; Brown, A. A.; Huck, W. T. S. UCST wetting transitions of polyzwitterionic brushes driven by self-association. *Angew. Chem., Int. Ed.* **2006**, *45*, 1770−1774.
(31) Cheng, N.; Brown, A. A.; Azzaroni, O.; Huck, W. T. S. Thickness-dependent properties of polyzwitterionic brushes. *Macromolecules* **2008**, *41*, 6317−6321.
(32) Draper, J.; Luzinov, I.; Minko, S.; Tokarev, I.; Stamm, M. Mixed polymer brushes by sequential polymer addition: Anchoring layer effect. *Langmuir* **2004**, *20*, 4064−4075.
(33) Ionov, L.; Minko, S.; Stamm, M.; Gohy, J. F.; Jerome, R.; Scholl, A. Reversible chemical patterning on stimuli-responsive polymer film: Environment-responsive lithography. *J. Am. Chem. Soc.* **2003**, *125*, 8302−8306.
(34) Forzani, E. S.; Perez, M. A.; Teijelo, M. L.; Calvo, E. J. Redox driven swelling of layer-by-layer enzyme-polyelectrolyte multilayers. *Langmuir* **2002**, *18*, 9867−9873.
(35) Palioura, D.; Armes, S. P.; Anastasiadis, S. H.; Vamvakaki, M. Metal nanocrystals incorporated within pH-responsive microgel particles. *Langmuir* **2007**, *23*, 5761−5768.
(36) Schmidt, D. J.; Cebeci, F. C.; Kalcioglu, Z. I.; Wyman, S. G.; Ortiz, C.; Van Vliet, K. J.; Hammond, P. T. Electrochemically Controlled Swelling and Mechanical Properties of a Polymer Nanocomposite. *ACS Nano* **2009**, *3*, 2207−2216.
(37) Mizutani, A.; Kikuchi, A.; Yamato, M.; Kanazawa, H.; Okano, T. Preparation of thermoresponsive polymer brush surfaces and their interaction with cells. *Biomaterials* **2008**, *29*, 2073−2081.
(38) Wu, T.; Gong, P.; Szleifer, I.; Vlcek, P.; Subr, V.; Genzer, J. Behavior of surface-anchored poly(acrylic acid) brushes with grafting density gradients on solid substrates: 1. Experiment. *Macromolecules* **2007**, *40*, 8756−8764.
(39) Parnell, A. J.; Martin, S. J.; Jones, R. A. L.; Vasilev, C.; Crook, C. J.; Ryan, A. J. Direct visualization of the real time swelling and collapse of a poly(methacrylic acid) brush using atomic force microscopy. *Soft Matter* **2009**, *5*, 296−299.
(40) Parnell, A. J.; Martin, S. J.; Dang, C. C.; Geoghegan, M.; Jones, R. A. L.; Crook, C. J.; Howse, J. R.; Ryan, A. J. Synthesis, characterization and swelling behaviour of poly(methacrylic acid) brushes synthesized using atom transfer radical polymerization. *Polymer* **2009**, *50*, 1005−1014.
(41) Pietrasik, J.; Sumerlin, B. S.; Lee, R. Y.; Matyjaszewski, K. Solution behavior of temperature-responsive molecular brushes prepared by ATRP. *Macromol. Chem. Phys.* **2007**, *208*, 30−36.
(42) Cheng, Z. P.; Zhu, X. L.; Shi, Z. L.; Neoh, K. G.; Kang, E. T. Polymer microspheres with permanent antibacterial surface from surface-initiated atom transfer radical polymerization. *Ind. Eng. Chem. Res.* **2005**, *44*, 7098−7104.
(43) Fielding, L. A.; Edmondson, S.; Armes, S. P. Synthesis of pH-responsive tertiary amine methacrylate polymer brushes and their response to acidic vapour. *J. Mater. Chem.* **2011**, *21*, 11773−11780.
(44) Topham, P. D.; Howse, J. R.; Crook, C. J.; Parnell, A. J.; Geoghegan, M.; Jones, R. A. L.; Ryan, A. J. Controlled growth of poly (2-(diethylamino)ethyl methacrylate) brushes via atom transfer radical

polymerisation on planar silicon surfaces. *Polym. Int.* **2006**, *55*, 808−815.
(45) Geoghegan, M.; Ruiz-Perez, L.; Dang, C. C.; Parnell, A. J.; Martin, S. J.; Howse, J. R.; Jones, R. A. L.; Golestanian, R.; Topham, P. D.; Crook, C. J.; Ryan, A. J.; Sivia, D. S.; Webster, J. R. P.; Menelle, A. The pH-induced swelling and collapse atom transfer radical polymerization. *Soft Matter* **2006**, *2*, 1076−1080.
(46) Moglianetti, M.; Webster, J. R.; Edmondson, S.; Armes, S. P.; Titmuss, S. Neutron Reflectivity Study of the Structure of pH-Responsive Polymer Brushes Grown from a Macroinitiator at the Sapphire− Water Interface. *Langmuir* **2010**, *26*, 12684−12689.
(47) Zhang, Y.; Lv, B. e.; Lu, Z.; He, J. a.; Zhang, S.; Chen, H.; Ma, H. Predicting Au−S bond breakage from the swelling behavior of surface tethered polyelectrolytes. *Soft Matter* **2011**, *7*, 11496.
(48) Witte, K. N.; Kim, S.; Won, Y.-Y. Self-Consistent Field Theory Study of the Effect of Grafting Density on the Height of a Weak Polyelectrolyte Brush. *J. Phys. Chem. B* **2009**, *113*, 11076−11084.
(49) Thomassin, J.-M.; Lenoir, S.; Riga, J.; Jerome, R.; Detrembleur, C. Grafting of poly 2-(tert-butylamino)ethyl methacrylate onto polypropylene by reactive blending and antibacterial activity of the copolymer. *Biomacromolecules* **2007**, *8*, 1171−1177.
(50) Banez, M. V. D.; Robinson, K. L.; Butun, V.; Armes, S. P. Use of oxyanion-initiated polymerization for the synthesis of amine methacrylate-based homopolymers and block copolymers. *Polymer* **2001**, *42*, 29−37.
(51) Morse, A. J.; Dupin, D.; Thompson, K. L.; Armes, S. P.; Ouzineb, K.; Mills, P.; Swart, R. Novel Pickering Emulsifiers based on pH-Responsive Poly(tert-butylaminoethyl methacrylate) Latexes. *Langmuir* **2012**, *28*, 11742−11753.
(52) Lenoir, S.; Pagnoulle, C.; Galleni, M.; Compere, P.; Jerome, R.; Detrembleur, C. Polyolefin matrixes with permanent antibacterial activity: Preparation, antibacterial activity, and action mode of the active species. *Biomacromolecules* **2006**, *7*, 2291−2296.
(53) Hoffmann, M.; Lang, M.; Sommer, J.-U. Gelation threshold of cross-linked polymer brushes. *Phys. Rev. E* **2011**, *83*.
(54) Huang, W. X.; Baker, G. L.; Bruening, M. L. Controlled synthesis of cross-linked ultrathin polymer films by using surface-initiated atom transfer radical polymerization. *Angew. Chem., Int. Ed.* **2001**, *40*, 1510−1512.
(55) Ahmad, S. A.; Leggett, G. J.; Hucknall, A.; Chilkoti, A. Micro- and nanostructured poly [oligo (ethylene glycol) methacrylate] brushes grown from photopatterned halogen initiators by atom transfer radical polymerization. *Biointerphases* **2011**, *6*, 8.
(56) Janssen, D.; De Palma, R.; Verlaak, S.; Heremans, P.; Dehaen, W. Static solvent contact angle measurements, surface free energy and wettability determination of various self-assembled monolayers on silicon dioxide. *Thin Solid Films* **2006**, *515*, 1433−1438.
(57) Alang Ahmad, S.; Hucknall, A.; Chilkoti, A.; Leggett, G. J. Protein Patterning by UV-Induced Photodegradation of Poly (oligo (ethylene glycol) methacrylate) Brushes. *Langmuir* **2010**, *26*, 9937−9942.
(58) Wu, T.; Efimenko, K.; Genzer, J. Combinatorial Study of the Mushroom-to-Brush Crossover in Surface Anchored Polyacrylamide. *J. Am. Chem. Soc.* **2002**, *124*, 9394−9395.
(59) Wu, T.; Efimenko, K.; Vlček, P.; Šubr, V.; Genzer, J. Formation and Properties of Anchored Polymers with a Gradual Variation of Grafting Densities on Flat Substrates. *Macromolecules* **2003**, *36*, 2448−2453.
(60) Jia, H.; Wildes, A.; Titmuss, S. Structure of pH-Responsive Polymer Brushes Grown at the Gold−Water Interface: Dependence on Grafting Density and Temperature. *Macromolecules* **2012**, *45*, 305−312.
(61) Moglianetti, M.; Webster, J. R. P.; Edmondson, S.; Armes, S. P.; Titmuss, S. Neutron Reflectivity Study of the Structure of pH-Responsive Polymer Brushes Grown from a Macroinitiator at the Sapphire-Water Interface. *Langmuir* **2010**, *26*, 12684−12689.
(62) Genzer, J. In silico polymerization: Computer simulation of controlled radical polymerization in bulk and on flat surfaces. *Macromolecules* **2006**, *39*, 7157−7169.
(63) Edmondson, S.; Vo, C.-D.; Armes, S. P.; Unali, G.-F. Surface polymerization from planar surfaces by atom transfer radical polymerization using polyelectrolytic macroinitiators. *Macromolecules* **2007**, *40*, 5271−5278.
(64) Edmondson, S.; Nguyen, N. T.; Lewis, A. L.; Armes, S. P. Co-nonsolvency effects for surface-initiated poly (2-(methacryloyloxy) ethyl phosphorylcholine) brushes in alcohol/water mixtures. *Langmuir* **2010**, *26*, 7216−7226.
(65) Thompson, K. L.; Bannister, I.; Armes, S. P.; Lewis, A. L. Preparation of Biocompatible Sterically Stabilized Latexes Using Well-Defined Poly (2-(methacryloyloxy) ethyl phosphorylcholine) Macromonomers. *Langmuir* **2009**, *26*, 4693−4702.
(66) Kim, J.-B.; Bruening, M. L.; Baker, G. L. Surface-Initiated Atom Transfer Radical Polymerization on Gold at Ambient Temperature. *J. Am. Chem. Soc.* **2000**, *122*, 7616−7617.
(67) Ding, S. J.; Floyd, J. A.; Walters, K. B. Comparison of Surface Confined ATRP and SET-LRP Syntheses for a Series of Amino (Meth)acrylate Polymer Brushes on Silicon Substrates. *J. Polym. Sci., Part A* **2009**, *47*, 6552−6560.
(68) Kaholek, M.; Lee, W. K.; Feng, J. X.; LaMattina, B.; Dyer, D. J.; Zauscher, S. Weak polyelectrolyte brush arrays fabricated by combining electron-beam lithography with surface-initiated photopolymerization. *Chem. Mater.* **2006**, *18*, 3660−3664.
(69) Moglianetti, M.; Webster, J. R. P.; Edmondson, S.; Armes, S. P.; Titmuss, S. A Neutron Reflectivity Study of Surfactant Self-Assembly in Weak Polyelectrolyte Brushes at the Sapphire-Water Interface. *Langmuir* **2011**, *27*, 4489−4496.
(70) Jia, H.; Grillo, I.; Titmuss, S. Small angle neutron scattering study of polyelectrolyte brushes grafted to well-defined gold nanoparticle interfaces. *Langmuir* **2010**, *26*, 7482−7488.